# Synthesis, physical and thermodynamic properties of lactic acid and malic acid based natural deep eutectic solvents

*Vânia I. B. Castro[1,2], Francisca Mano[3], Margarida S. Miranda[1,2], Rui L. Reis[1,2,4], Alexandre Paiva[3], Ana Rita C. Duarte[1,2,3]**

1_3B's Research Group – Biomaterials, Biodegradables and Biomimetics, University of Minho, Headquarters of the European Institute of Excellence on Tissue Engineering and Regenerative Medicine, Avepark 4805-017 Barco, Guimarães, Portugal.

2_ICVS/3B's PT Government Associated Laboratory, Braga/Guimarães, Portugal.

3_ LAQV-REQUIMTE, Departamento de Química, Faculdade de Ciências e Tecnologia, Universidade Nova de Lisboa, 2829-516 Caparica, Portugal.

4_The Discoveries Centre for Regenerative and Precision Medicine, Headquarters at University of Minho, Avepark 4805-017 Barco, Guimarães, Portugal.

ABSTRACT

In this paper, four natural deep eutectic solvents (NADES) systems were prepared at specific molar ratios, La:Bet (2:1) (lactic acid:betaine), La:Hist (9:1) (lactic acid:histidine), Ma:Bet:$H_2O$ (1:2:3) (malic acid:betaine:water) and Ma:Bet:Pro:$H_2O$ (1:1:1:2) (malic acid:betaine:proline:water). Their physical and thermodynamic properties were studied, namely viscosity, electrical conductivity, heat capacity and vapor pressure. The viscosity and electrical conductivity were determined as function of temperature and the correlation for the temperature dependence was obtained and discussed based on Arrhenius theory. The heat capacity for all eutectic systems was measured by differential scanning calorimetry (DSC) over a temperature range of 293.15 K to 363.15 K. The vapor pressure La:Bet (2:1) and La:Hist (9:1) was determined by thermogravimetric analysis (TGA). The ability of these NADES to reduce cellulose crystallinity was evaluated. Cellulose crystallinity after suspension in these NADES was studied by X-ray diffraction. Cellulose suspended in Ma:Bet:$H_2O$ (1:2:3) suffer the highest crystallinity reduction among the systems studied and was about of 20%.

## 1. INTRODUCTION

Green chemistry presents itself as the most active field of science to develop sustainable processes and/or solvents.[1–4] In an Era where, industrial growing has been exponential, this has a significant negative impact on the environment. With this, several alternatives of processes and compounds/solvents have emerged as a strategy to reduce or minimize this negative impact. In the last decades, compounds as ionic liquids (IL) have been present as such alternative solvents, but it has been verified that these solvents have some drawbacks as high cost of synthesis, purification requirements and toxicity. More recently, a new type of solvents have emerged called Deep Eutectic Solvents (DES).[5–9] DES are formed by two or three components/compounds which are capable to interact, through hydrogen bonds and/or electrostatic interaction and hence create an eutectic mixture.[2,10–13] The main characteristic of DES is that the melting point of the mixture is much lower when compared with each individual component. In some cases, a very large depression of the melting point is observed, being the mixture liquid at room temperature.[3,8,14]

Several investigations, regarding plant and animal metabolism, report a large number of stable compounds composed of primary metabolites, which were found to have similar properties to DES. Due to their natural occurrence these systems are called Natural Deep Eutectic Solvents (NADES). NADES are, thus, defined as a mixture of two or more components of natural origin such as sugars, carboxylic acids, alcohols and amino acids.[1,8,15–17] NADES present all characteristics for which a green solvent is recognized. This family of compounds presents several advantages such as ease to prepare with high purity and high yield. These eutectic systems are also known to be non-toxic, biodegradable, biocompatible and present a low vapor pressure.[3,6,8,10,17–19]

Industrial applications of NADES are very promising namely organic synthesis,[8.12.15] extraction processes,[15,20,21] electrochemistry[16,22,23] and enzymatic reactions[24–28] among others.

Some eutectic systems have already demonstrated the potential to dissolve lignocellulosic material. Lignin, hemicellulose, cellulose and starch solubility was evaluated and successfully demonstrated.[29]

In this work the DES systems will be characterized to fully understand them and also to allow the design and development of models able to predict their properties.[3,5,6,15] The ability of these systems as modifiers of cellulose crystallinity will also be tested.

## 2. EXPERIMENTAL

### 2.1. Materials

The chemical reagents L-Histidine (CAS 71-00-1), L-Proline (CAS 147-85-3) and Betaine (CAS 107-43-7) were acquired from Sigma-Aldrich with a purity of 99.8%. 99.9% and 99.0%, respectively. Cellulose fibers (CAS 9004-34-6) was also purchased from Sigma-Aldrich.

DL-lactic acid (CAS 50-21-5) was acquired from TCL with a purity of 85.0% and DL-malic acid (6915-15-7) was acquired from Alfa-Aesar with a purity of 98%.

For the thermogravimetric measurements it was used hexadecane (CAS 544-76-3), bought from Sigma-Aldrich with a purity of 99.8%. Table 1 lists the chemical reagents used.

**Table 1.** Names, sources, and purities of chemicals used in the current study chemical.

| Chemical | Physical state | source | assay | CAS registry number |
|---|---|---|---|---|
| L-Histidine | solid | Sigma-Aldrich | 99.8% | 71-00-1 |
| L-Proline | solid | Sigma-Aldrich | 99.9% | 147-85-3 |
| Betaine | solid | Sigma-Aldrich | 99.0% | 107-43-7 |
| Cellulose fibers | solid | Sigma-Aldrich | | |
| Hexadecane | liquid | Sigma-Aldrich | 99.8% | 544-76-3 |
| Water ultrapure | liquid | System Milli-Q | | |

| | | | | |
|---|---|---|---|---|
| DL-lactic acid | liquid | TCL | 85.0% | 50-21-5 |
| DL-malic acid | solid | Alfa-Aesar | 98.0% | 6915-15-7 |

### 2.2. Preparation of the NADES

The NADES were prepared by the heating and stirring method. This method consists in mixing the components of the mixture (two or more), according to the amounts calculated considering different molar ratios (Table 2). The systems were heated to 343.15 K and stirred at 300 rpm, until a clear liquid is formed (1h30-2h). A 831 KF Coulometer with generator electrode and without diaphragm was used. The water content values given are an average of at least three measurements.

### 2.3. Polarized light microscopy (POM)

The optical characterization of NADES samples was performed at room temperature by POM, using an Olympus transmission microscope (Olympus, UK) coupled with a Leica digital camera DFC 280 (Leica, UK). Microscope slides containing 1-2 droplet of the different NADES prepared were observed under the microscope under polarized light.

### 2.4. Differential scanning analysis (DSC)

#### 2.4.1 Assessment of heating profile/degradation temperature

The NADES and initial components were characterized by DSC (model DSC Q100, T.A, instruments, USA) in a temperature range of 233.15 K up to the degradation temperature, at a heating rate of 5 K $min^{-1}$, after an isothermal period at 233.15 K of 5 min. The analyses were performed under nitrogen atmosphere (50 mL $min^{-1}$) with 10-15 mg of sample of NADES in an aluminium pan with a covering lid.

#### 2.4.2 Measurement of molar heat capacity

For the measurement of the molar heat capacity ($C_p$) of NADES the same DSC equipment was used. For each run, a 5 min isothermal at 293.15 K was followed by a temperature ramp from 293.15 K to 363.15 K at a heating rate of 5 K $min^{-1}$, and then a final isothermal stage at 363.15 K for 5 min. The differential heat flow curve of the samples was compared with that of standard sapphire.[30] Both curves were blank corrected. Calibration of the equipment was performed using indium. The method used for measurement of the $C_p$ of NADES was validated by measuring the $C_p$ of ultrapure water. All measurements were replicated three times, and the averaged values±standard deviation were reported.

### 2.5. Measurement of conductivity

The conductivity (σ) was measured using an Inolab multi-level 3 (WTW) equipment equipped with a WTW Tetracon® 325 conductivity probe and with built-in temperature and conductivity sensors. For each system, the conductivity was measured in triplicate. The liquid (4 mL) was enclosed on a sealed bottle, fitted with the conductivity sensor. The system was immersed in a water bath, with temperature sensor for controlling temperature, at a temperature range of 293.15 K to 343.15 K. All measurements were replicated three times, and the averaged values±standard deviation were reported.

### 2.6. Measurement of viscosity

The viscosity of the systems was measured using a Kinexus Prot+ Rheometer (Kinuxus Pro t+, MaL 1097376, Malvern) equipped with the plate geometry with 20 mm of diameter (PU20 SR1740 SS) and the gap used was 1 mm. For each run, the method used consisted in an equilibrium step at 293.15 K during 5 min followed by a temperature ramp from 293.15 K to 344.15 K, at 5 K $min^{-1}$.

The viscosity, for each system, was measured three times and the results are presented as the average values ± standard deviation.

### 2.7. Simultaneous Thermal Analyzer – STA

The vapor pressure of La:Bet (2:1) and La:Hist (9:1) were determined by thermogravimetric analysis (TGA) using a STA - Simultaneous Thermal Analyser (STA7200, 10101018000033, Hitachi). The analyses were performed according to previously reported optimal experimental conditions.[31] A sample of about 50-60 mg of NADES was placed in a platinum crucible with vertical walls, a diameter of 5 mm and 2.5 mm height. The crucible was filled up to the edge. A nitrogen gas flow of 200 mL $min^{-1}$ was used. The temperature ranged from 333.21 K to 389.01 K for La:Bet (2:1) and from 332.91 K to 388.27 K for La:Hist (9:1) and a heating rate of 1 K $min^{-1}$ was used. The mass loss at each isothermal step of the scan was of 0.2-0.8 mg, the duration of each isothermal step was of at least 10 min and the temperature range used for each NADES was of 60 K. The samples inside the TGA were carefully conditioned. Each NADES was exposed to a heating ramp of 5 K $min^{-1}$ until 383.15 K for 20 min. This procedure allowed the removal of volatile impurities and traces of water. This heating ramp was repeated until a reproducible mass loss within two consequent runs was recorded.

The NADES incorporating water (Ma:Bet:$H_2O$ (1:2:3) and Ma:Bet:Pro:$H_2O$ (1:1:1:2)) were not studied using this TGA method as the temperatures used to evaporate the samples would be above the boiling temperature of water and this fact could influence the composition of the NADES.

To test the selected experimental conditions for the determination of the vapor pressure of the NADES we have studied one compound (hexadecane) which has well-established vapor pressure in order to confidently extend this condition to the NADES for which there is no experimental

data. The obtained results were compared to those described in the literature.[32,33] For each compound at least 7 independent runs have been performed in the selected temperature range.

### 2.8. Crystallinity of cellulose after NADES treatment.

To determine the effect of NADES in the reduction of cellulose crystallinity, long cellulose fibers or cotton linters were used, as an example of this polymer. In a vial 20 mg of cellulose was weighed and 1 g of each NADES was added. The suspensions were stirred overnight at 313.15 K. For the Ma-based NADES experiments were also performed at 333.15 K.

After that period, cellulose was recovery by water precipitation, centrifuged and washed three times with ethanol, to assure all DES removal. The recovered cellulose was dried and the crystallinity analyzed through X-ray diffraction method.

### 2.9. X-ray diffraction method

The XRD patterns were collected using a conventional Bragg–Brentano diffractometer (Bruker D8 Advance DaVinci, Germany) equipped with CuKα radiation, produced at 45 kV and 36 mA. Data sets were collected in the 2θ range of 5-50º with a step size of 0.05º and 15s for each step.

For crystallinity reduction determination (CR), the deconvolution method was used.[34] The peak integration was done with the help of Fit Peak, from Origin (OriginLab, Northampton, MA). The crystallinity reduction (CR) of cellulose and cellulose NADES-treated was determined according to the following equation:

$$CR\ (\%) = \frac{CI_{cellulose} - CI_{sample}}{CI_{cellulose}}, \quad (1)$$

whereas CI is the crystallinity index (%) that is determined from the ratio of the area of all crystalline peaks to the total area.

3. RESULTS AND DISCUSSION

### 3.1. NADES preparation

In the present work four NADES were prepared. These NADES are composed by acids and amino acids (Figure 1) in the adequate molar ratio to form the eutectic mixture, and they are liquid at room temperature. The eutectic systems herein studied are La:Bet (2:1), La:Hist (9:1), Ma:Bet:$H_2O$ (1:2:3) and Ma:Bet:Pro:$H_2O$ (1:1:1:2). The eutectic systems were obtained by mixing the components of each system in the correct/appropriate molar ratio. While malic acid based systems required the addition of water to form the viscous and transparent liquid NADES at room temperature, in turn, the lactic acid based systems do not require the addition of water. However, Karl Fisher titration has shown that water is present in the systems La:Bet (2:1), La:Hist (9:1) and the ratio of water present in these systems was determined to be La:Bet:$H_2O$ (2:1:2) and La:Hist:$H_2O$ (9:1:5). The values obtained for each NADES thourgh Karl Fischer are shown in table S1. Table 2 lists the components that constitute the NADES systems and the molar masses that were determined for each eutectic system.

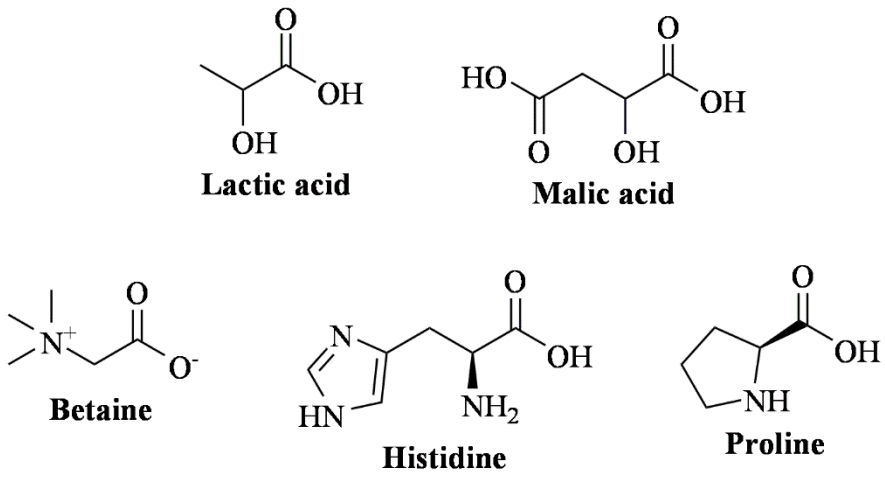

**Figure 1.** Chemical structure of the components used to prepare the natural deep eutectic solvents (NADES).

Throughout the preparation process, the systems acquired the liquid form after few hours (1h30-2h). The systems present a clear, limpid and transparent liquid and without evident crystals present. After cooling this aspect is maintained, the systems are stable and no precipitates were observed. All properties were determined for the systems La:Bet:$H_2O$ (2:1:2), La:Hist: $H_2O$ (9:1:5), Ma:Bet:$H_2O$ (1:2:3) and Ma:Bet:Pro:$H_2O$ (1:1:1:2), with the exception of the vapor pressure. In this case the systems La:Bet:$H_2O$ (2:1:2) and La:Hist: $H_2O$ (9:1:5) were studied, but we ensured the complete drying.

**Table 2.** Description of the components that comprise the NADES studied and molar ratios.

| NADES | Component 1 | Component 2 | Component 3 | Component 4 | Molar ratio[a] | Molar mass $M_{NADES}$[b] (g $mol^{-1}$) |
|---|---|---|---|---|---|---|
| La:Bet:$H_2O$ | Lactic acid | Betaine | Water[c] | _ | 2:1:2 | 66.67 |
| La:Hist:$H_2O$ | Lactic acid | Histidine | Water[c] | _ | 9:1:5 | 70.40 |
| Ma:Bet:$H_2O$ | Malic acid | Betaine | Water | _ | 1:2:3 | 70.41 |

| | | | | | | |
|---|---|---|---|---|---|---|
| Ma:Bet:Pro:$H_2O$ | Malic acid | Betaine | Proline | Water | 1:1:1:2 | 80.48 |

[a] Standard uncertainty, *u*, in mole fraction are u(x) = 0.001.

[b] $M_{NADES} = x_{comp1}M_{comp1}+\ldots+ x_{comp4}M_{comp4}$, where *x* and M are mole fraction and molar mass, respectively;

[c] The water content was not added to the system, it is present in the lactic acid raw material.

### 3.2. POM and DSC results

The POM characterization (Figure 2) confirms the successful production of these four eutectic systems as the mixtures did not contain any crystals.

The thermal behaviour was studied by DCS. The thermograms for La:Bet:$H_2O$ (2:1:2), La:Hist:$H_2O$ (9:1:5), Ma:Bet:$H_2O$ (1:2:3) and Ma:Bet:Pro:$H_2O$ (1:1:1:2) mixtures and the individual components are presented in Figure 3. The thermograms of the eutectic mixtures did not present any of the characteristic peaks (i.e., melting points) of the pure components.

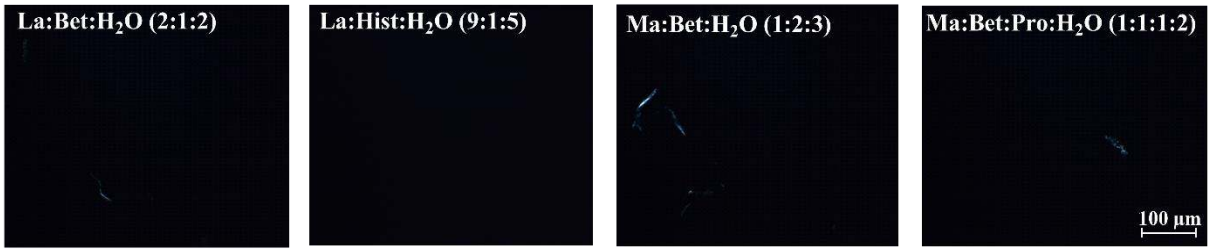


**Figure 2.** POM images of NADES, at 293.15 K.

These systems presented a high stability, the mixtures stayed in liquid form and without crystals precipitated for at least 12 months. This stability can be related with the number of hydrogen bond donor or acceptor groups, the spatial structure of those groups as well as the position of the bonds.[3,35]

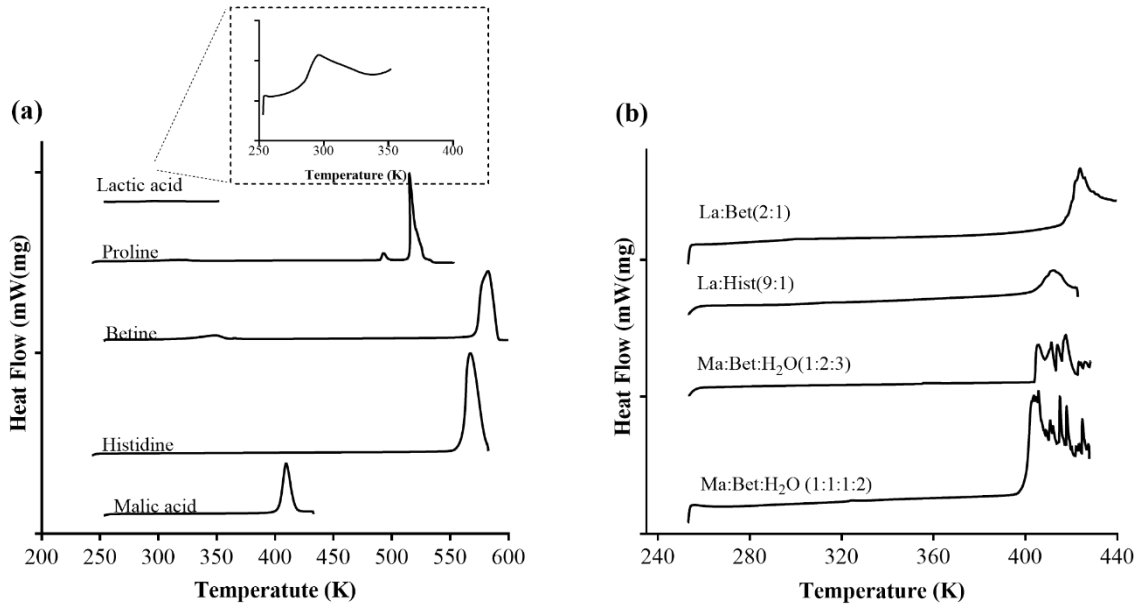


**Figure 3.** DSC thermograms of raw materials (a) and eutectic systems (b).

### 3.3. Viscosity and Conductivity

The chemical nature of the NADES components affects their thermophysical properties, as viscosity and conductivity. In the present work, the viscosity was measured in a temperature range from 293.15 K to 344.15 K. In Figure 4(a) it is possible to observe the influence of temperature in the viscosity of the NADES. The results (Table S2) show that there is a high variation in the viscosity with temperature, which points out that the properties of NADES are extremely sensitive to temperature. This is particularly important for the development of new processing technologies and the use of NADES. The viscosity of all the NADES decreased with the increase in temperature, as the internal resistance of the molecules decreases and the molecules more easily flow and the liquid is thus less viscous.[36,37]

The high viscosity of NADES are often attributed to the presence of hydrogen bonds in the network but also to Van der Walls and electrostatic interactions.[13,36,38,39] The viscosity is also

influenced by the molar ratio and the number of components that form the eutectic systems. Just like in the IL's in the DES, the internal resistance of a fluid at shear stress and intermolecular interactions are the main influence of the viscosity values obtained. DES and Il´s also share the feature of the to present higher viscosities than other molecular solvents and their differences are associated at hydrogen interactions.[40–43]

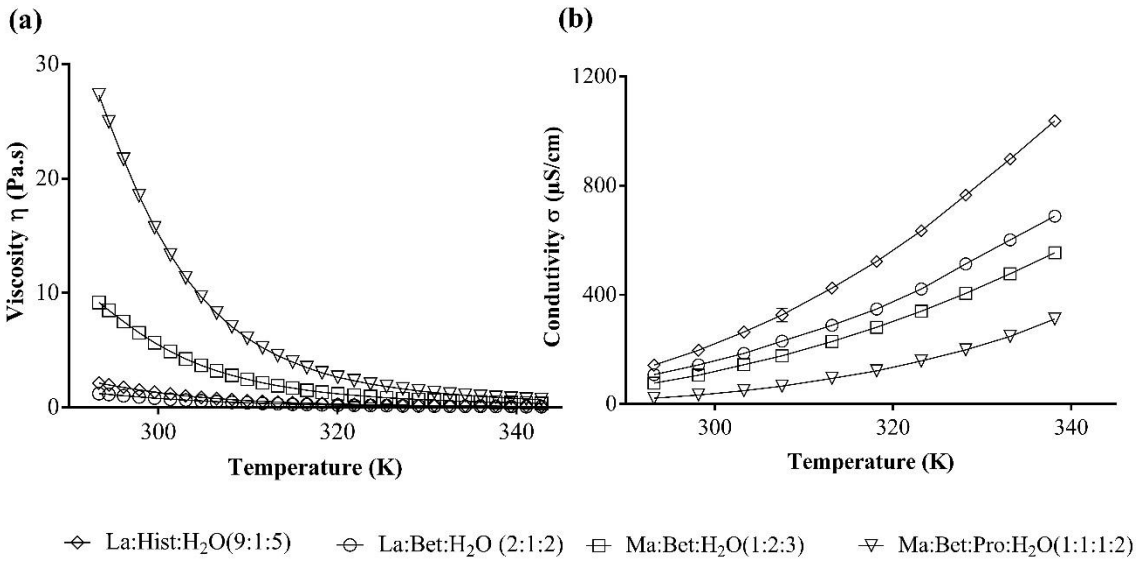


**Figure 4.** Viscosity (a) and conductivity (b) as function of temperature for the four different NADES studied.

Ma:Bet:Pro:$H_2O$ (1:1:1:2) is a system with higher molar ratio and with more components tends to present a higher viscosity, because the viscosity is influenced by the number of interactions between the components. If there are more components the number of interactions increases and therefore the viscosity will increase.[13,37,39,44] These intrinsic properties of NADES explain the higher viscosity at 298 K. The NADES Ma:Bet:Pro:$H_2O$, with 1:1:1:2 molar ratio and more components (four), is the more viscous NADES. This might be due to the large amount of hydrogen bond network that is formed between the components. On the other hand, the NADES

La:Bet:$H_2O$ with a 2:1:2 molar ratio is the less viscous mixture. Therefore, we have the following sequence: Ma:Bet:Pro:$H_2O$ (1:1:1:2) > Ma:Bet:$H_2O$ (1:2:3) > La:Hist: $H_2O$ (9:1:5) > La:Bet: $H_2O$ (2:1:2 ) (2:1), from more viscous to less viscous system, as it is possible to see in Figure 4(a).

**Table 3.** Linear regression fitting parameters for viscosity and conductivity, in the temperature (T) range of 298.15 – 343.15 K for four DES at 101.3 kPa.

| NADES | Viscosity | | | Conductivity | | |
|---|---|---|---|---|---|---|
| | $E_\eta$ (kJ mol$^{-1}$) | Ln $\eta_0$ | $R^2$ | $E_\sigma$ (kJ mol$^{-1}$) | Ln $\sigma_0$ | $R^2$ |
| La:Bet:$H_2O$ (2:1:2) | 49.64 | -20.17 | 0.9990 | 33.80 | 18.62 | 0.9966 |
| La:Hist:$H_2O$ (9:1:5) | 55.01 | -21.83 | 0.9984 | 36.07 | 19.85 | 0.9940 |
| Ma:Bet:$H_2O$ (1:2:3) | 55.85 | -20.74 | 0.9968 | 35.77 | 19.11 | 0.9933 |
| Ma:Bet:Pro:$H_2O$ (1:1:1:2) | 63.68 | -22.86 | 0.9968 | 48.35 | 23.02 | 0.9933 |

The conductivity of the four NADES was measured in a temperature range from 293.15 K to 344.15 K (Figure 4(b) and Table S3). The conductivity is related to ion mobility, this is, as the ion mobility increases, the conductivity increases[13,27,31,32] and it is affected by the number of charged species and their mobility, hence, highly viscous systems have a low conductivity. The conductivity follows the sequence: Ma:Bet:Pro:$H_2O$ (1:1:1:2) < Ma:Bet:$H_2O$ (1:2:3) < La:Bet: $H_2O$ (2:1:2) < La:Hist: $H_2O$ (9:1:5), from the system with lower conductivity to the system with higher conductivity. This is confirmed in Figure 4(b). The conductivity of NADES is also greatly influenced by temperature, namely, the conductivity increases significantly with increasing temperature. Conductivity, being related with the viscosity of the system behaves oppositely. While increasing temperature decreases the viscosity of the system, it causes a faster movement of the ions, thus increased conductivity. In this sense, systems less viscous have higher

conductivity.[13,27,31,32] However, in the La based NADES there is an apparent change in the order, La:Hist:$H_2O$ (9:1:5), has higher viscosity than La:Bet:$H_2O$ (2:1:2) but the conductivity is a slightly superior to the La:Bet:$H_2O$ (2:1:2). On the other hand, the Ma based NADES present a behaviour as expected, the more viscous system (Ma:Bet:Pro:$H_2O$ (1:1:1:2)) presents a lower conductivity.

The variation of viscosity with temperature can be expressed through the logarithmic form of Arrhenius equation as shown below:

$$ln\eta = ln\eta_0 + \frac{E_\eta}{RT} \quad (2)$$

Where $\eta$ is the viscosity, $\eta_0$ is a constant and $E_\eta$ is the flow activation energy, R is the gas constant and $T$ is the absolute temperature. The activation energy describes the potential barrier that ions must overcome to move past the other. Therefore, the higher the activation energy the more difficult to the ions to move past each other. In this work, the estimated values of activation energy were from 49.64 kJ mol$^{-1}$ to 63.68 kJ mol$^{-1}$, which are in agreement with the reported values in the literature for other DES.[36,47]

Similarly, and as observed for viscosity, the dependence of conductivity with temperature can also be expressed in the logarithmic form of Arrhenius equation as show below:

$$\ln\sigma = \ln\sigma_0 + \frac{E_\sigma}{RT} \quad (3)$$

Where $\sigma$ is the conductivity, $\sigma_0$ is a constant and $E_\sigma$ is the activation energy for electrical conduction, R is the gas constant and $T$ is the absolute temperature. Table 3 presents the summarized values of $E\sigma$ for four NADES. In this work, the estimated values of activation energy are between 33.80 kJ mol$^{-1}$ and 48.35 kJ mol$^{-1}$, which correlate/agrees with the reported values in the literature for other DES.[12,45,47–49]

As aforementioned, the conductivity is usually governed by the mobility of charged species in ionic fluids, therefore the conductivity will be proportional to the fluidity ($\eta^{-1}$) of the system.

Figure 5 shows the linear correlation between conductivity and the reciprocal of viscosity. This linear correlation indicates that the conductivity of the liquid mixtures is limited by the ionic mobility.

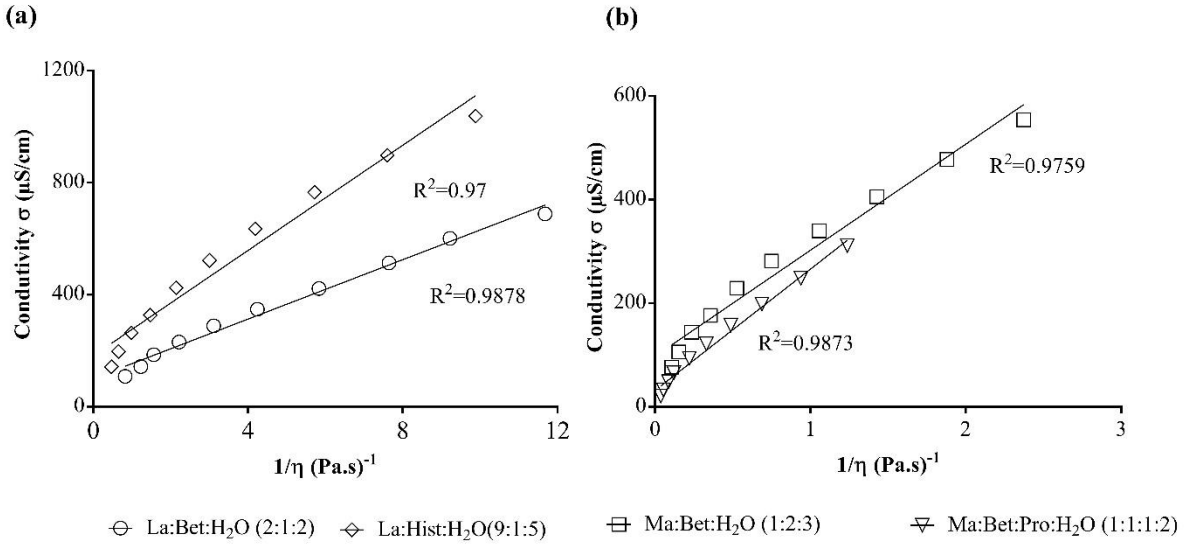


**Figure 5.** Conductivity as a function of fluidity ($\eta^{-1}$) for four NADES, La based NADES (a) and Ma based NADES (b).

### 3.4. Molar heat capacity ($C_p$)

The molar heat capacity ($C_p$) of the NADES was determined by DSC at a temperature range from 293.15 K to 363.15 K. The values of $C_p$ are presented in Figure 6 and Table S4. It can be observed that for the studied NADES the values of the $C_p$ linearly and slightly increase with increasing temperature.

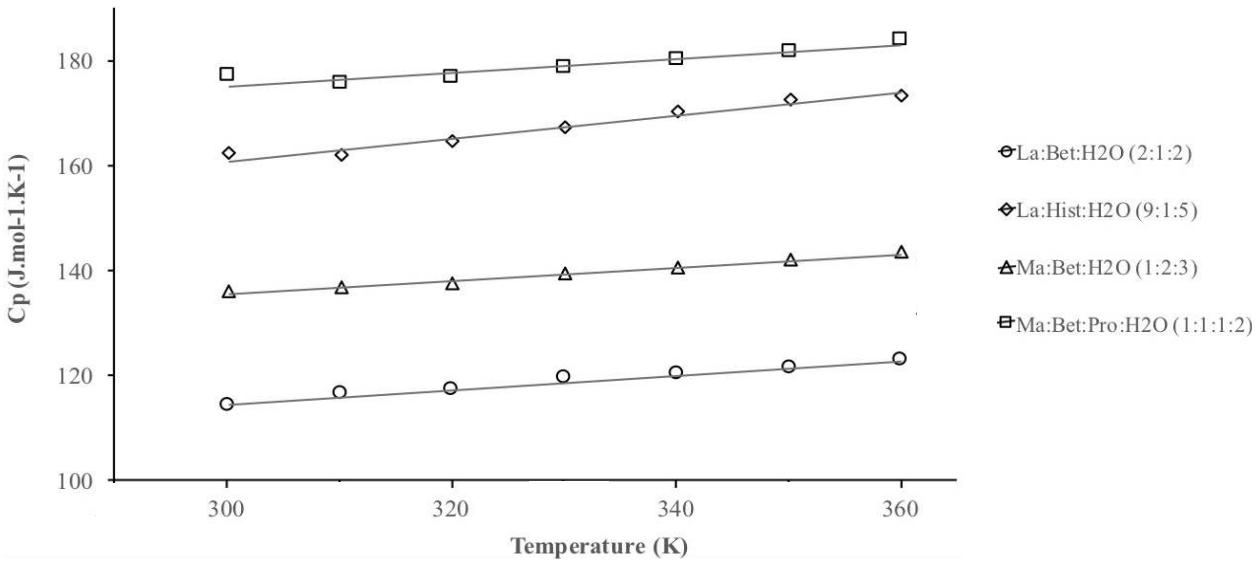


**Figure 6.** Molar heat capacity for the four different NADES as a function of temperature.

The $C_p$ of NADES were correlated with temperature using a linear equation given as equation (4):

$$C_p(J\ mol^{-1}K^{-1}) = a_0 + a_1T(K) \quad (4)$$

Where $T$ is the absolute temperature, and $a_0$ and $a_1$ are adjustable parameters obtained by applying the least-squares method (Table 4). Herein, the applied correlation yields a good estimate of the $C_p$ of the four NADES, as can be seen in Figure 6. The average absolute deviation (AAD) between the experimental and calculated values was calculated from equation (5):

$$AAD(\%) = \frac{100}{n} * \sum_{i=1}^{n} \left| \frac{C_{p,i}^{exp} - C_{p,i}^{pred}}{C_{p,i}^{exp}} \right| \quad (5)$$

Where $C_{p,i}^{exp}$ and $C_{p,i}^{pred}$ are the experimental and calculated values, respectively.

It can also be noted that for the same temperature, the $C_p$ of La:Bet:$H_2O$ (2:1:2), is lower than La:Hist:$H_2O$ (9:1:5), moreover it is higher than of Ma:Bet:$H_2O$ (1:2:3) and it is higher than of Ma:Bet:Pro:$H_2O$ (1:1:1:2), which indicates that $C_p$ decreases with increasing NADES molar mass ($M_{NADES}$) (Table 2). This behaviour is attributed to the number of motion degrees of freedom that

are available to the particles in the substance. These results correlate with the reported values in the literature for other DES/NADES.[45,50–53]

**Table 4.** Fitting parameters of equation (4) for the $C_p$ of the different NADES.

| NADES | Parameter | | No. of data points. n | AAD (%) |
|---|---|---|---|---|
| | $a_0$ | $a_1$ | | |
| La:Bet:$H_2O$ | 0.1365 | 73.559 | 7 | 0.05 |
| La:Hist:$H_2O$ | 0.216 | 96.176 | 7 | 0.09 |
| Ma:Bet:$H_2O$ | 0.127 | 97.290 | 7 | 0.07 |
| Ma:Bet:Pro:$H_2O$ | 0.132 | 135.340 | 7 | 0.17 |
| | | | 28 | 0.10 |

### 3.5. Vapor pressure

The TGA experiments performed also allow the determination of the values of vapor pressure. Langmuir equation can be rearranged as follows to determine the vapor pressure:[31,32]

$$p = k\nu \tag{6}$$

Where

$$k = \frac{\sqrt{2\pi R}}{\alpha} \tag{7}$$

And

$$\nu = \left(\frac{dm}{dt}\right)\sqrt{\frac{T}{M}} \tag{8}$$

where *dm/dt* is the rate of mass loss, *p* is vapor pressure, M is molecular mass of the evaporating substance, R is the gas constant, *T* is temperature and α is the evaporation coefficient. The hexadecane was selected to determine the constant *k*. Once the constant *k* was determined the vapor pressure of NADES was calculated using equation (8) by means of the measured evaporation rates,

under the same experimental conditions. For hexadecane, the evaporation rate at a temperature range of 350.90 K to 417.78 K and the values are reported in Table S5. Subsequently, the parameter ν was calculated from equation (10) and in Figure S1 is presented a plot of vapor pressure ($p$) of hexadecane against the ν calculated in this work. As it can be observed, there is a linear relationship between $p$ and ν from which the $k$ was determined as $-8.2 \times 10^6$.

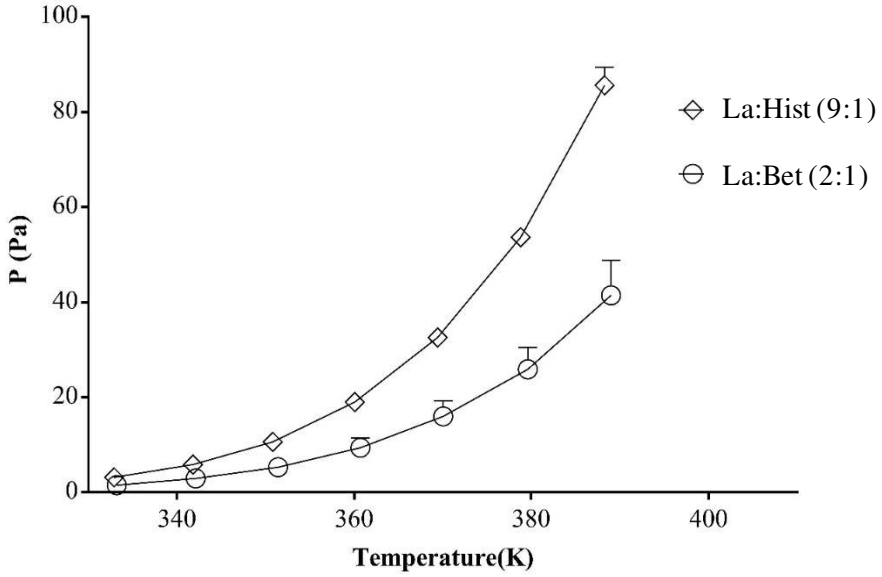


**Figure 7.** Vapor pressure of La based NADES.

The vapor pressure of NADES was obtained from equation (8) by measuring their evaporation rates. Table S6 shows the evaporation rates measured, calculated ν and vapor pressures of the NADES at 330.15 K to 390.15 K. As it is expected the vapor pressures of NADES increases with the increase of temperature Figure 7.

Studies about the vapor pressure of NADES have demonstrated that the formation of hydrogen bonds decreases the vapor pressure.[11,33,54,55] As aforementioned, hydrogen bonding also influences the viscosity of the system, likewise, more viscous systems present lower vapor pressures.[31,33]

### 3.6. Crystallinity reduction of cellulose treated with DES

The ability of using cellulose as subtract in an enzymatic reaction is very reduced, due to its supramolecular structure. Only few enzymes are capable of degrading cellulose into more simple sugars. Consequently, it is essential to modified cellulose crystallinity, as an attempt to empowering cellulases' competence, reducing the reaction kinetics' as well.

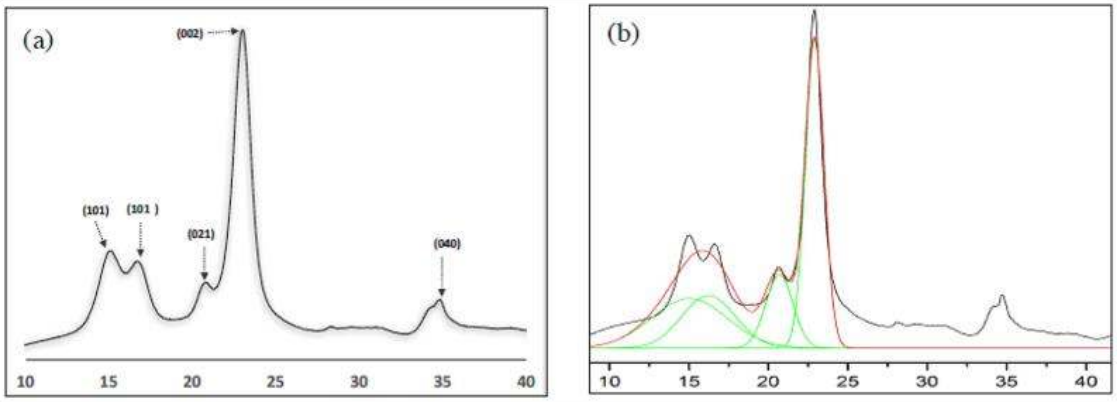


**Figure 8.** Cellulose diffraction plans (a) and an example of the Gaussian function applied to the diffractogram for the deconvolution method (b).

The ability of using NADES as modifiers of cellulose crystallinity has been reported in the literature. However, its effect has not yet been quantified.[29]

The crystallinity quantification was performed by X-RAY analysis. The cellulose crystallinity diffractions plans: 101, $10\bar{1}$, 021, 002 and 040, represented in Figure 8 (a) where used to determine the crystallinity of the samples. Following the deconvolution method (one example of this method is shown on Figure 8(b)), a Gaussian function was assumed for each peak and each was individually integrated with Fit Peak software. The total area was also determined using the same software.

From $CR\ (\%) = \frac{CI_{cellulose} - CI_{sample}}{CI_{cellulose}}$, (9)

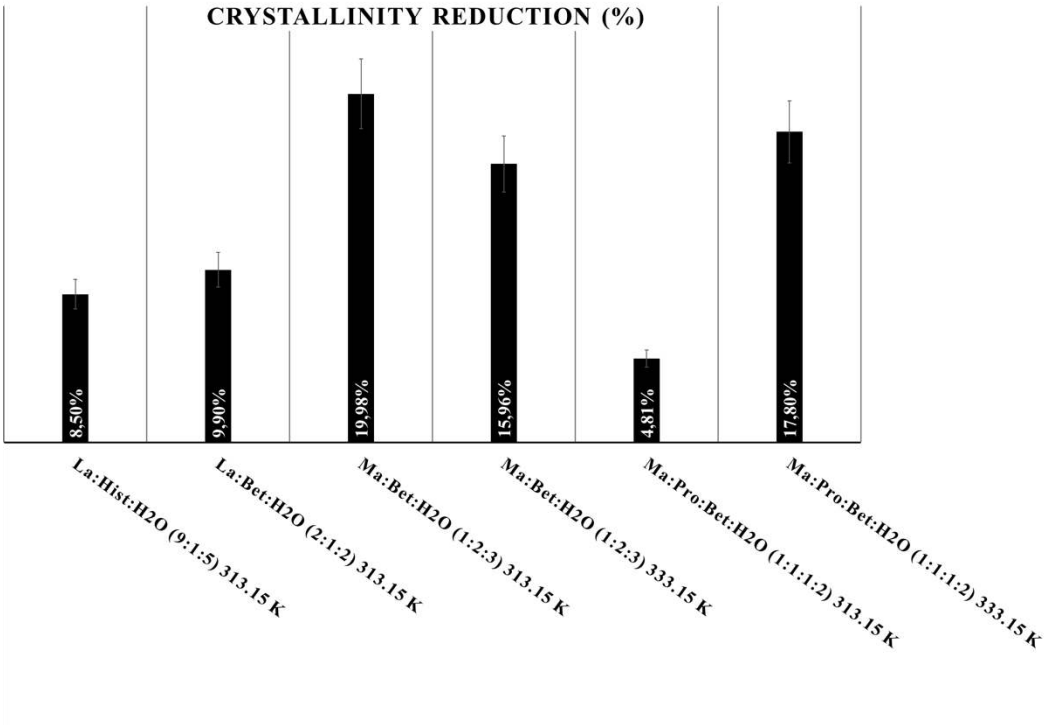


**Figure 9.** Crystallinity reduction calculated for the DES systems used, at different temperatures.

The cellulose crystallinity reduction was determined, and the effect of each NADES used was studied. The results obtained are shown in Figure 9. According to the values obtained, NADES show promising results in changing the supramolecular structure of cellulose. MA-based NADES seem to have a higher influence on the reduction of cellulose crystallinity. In the case of Ma:Bet:Pro:$H_2O$ (1:1:1:2), at 313.5 K the CR value obtained can be justified with the solvent viscosity at that temperature. In Figure 4 it is possible to observe that this NADES is the one with the higher viscosity value. It is only after 330 K that Ma:Bet:Pro:$H_2O$ (1:1:1:2) reaches the same viscosity values as the other NADES studied. Consequently, lower viscosity values may improve DES-cellulose interactions, leading to higher crystallinity reduction, as shown in

Figure **9**. One other hand, systems with lower viscosities also demonstrate lower crystallinity reductions, being the case of La:Hist:$H_2O$ (9:1:5) and La:Bet:$H_2O$ (2:1:2).

## 4. CONCLUSIONS

In this study, four new NADES were prepared and characterized by POM and DSC. The characterization demonstrated that these NADES, at room temperature, are viscous liquids and present low conductivity. However, this study also demonstrated that with the increase of temperature, viscosity decreases while the conductivity increases. As both properties are dependent on the temperature it was possible to model the systems after the logarithmic form of the Arrhenius equation. The molar heat capacity and vapor pressure were calculated for the NADES studied. It was possible to confirm that the molar heat capacities increased with increasing molar mass of NADES. It was also possible to correlate the viscosity with vapor pressure, and according to our experiments the more viscous systems present lower vapor pressures. All measured physical and thermodynamic properties demonstrated to be influenced by temperature and by the hydrogen bonds characteristic of these type of systems. The determination of these properties of NADES is surely useful towards their potential industrial applications, namely to understand the reduction of cellulose crystallinity, as presented here. It was shown that all NADES were able to reduce the crystallinity of cellulose achieving a maximum reduction of 20% in crystallinity for the case of cellulose suspended in Ma:Bet:$H_2O$ (1:2:3) at 313.15 K. From this work it was possible to prove that cellulose crystallinity can be modified, opening new opportunities for the application of these solvents. By using NADES as a pre-treatment or even as potential one-pot reaction, it will be possible to reduce time and process costs on degrading cellulose through enzymes.

## AUTHOR INFORMATION

**Corresponding Author**

*aduarte@fct.unl.pt

## Author Contributions

V.I.B.C. and F.M. prepared the NADES. V.I.B.C. conducted the experiments of characterization of NADES. V.I.B.C. and M.S.M. realized the TGA experiments. F.M. conducted the experiments reduction of cellulose crystallinity. A.P., A.R.C.D., F.M. M.S.M. and V.I.B.C. analysed the data and participated in the interpretation of results. All authors have read and approved the final manuscript.


## Funding Sources

The research leading to these results has received funding provided by Fundação para a Ciência e a Tecnologia through the project PTDC/BBB-EBB/1676/2014 – DesZyme. Funding from the European Union, Horizon 2020 program has also been granted through project Des.solve (ERC consolidator) ERC-2016-COG 725034. This work was supported by the Associate Laboratory for Green Chemistry- LAQV which is financed by national funds from FCT/MCTES (UID/QUI/50006/2013) and co-financed by the ERDF under the PT2020 Partnership Agreement (POCI-01-0145-FEDER - 007265). The authors would like to acknowledge Sandra Pina and Isabel Leonor for help provided in the XRD analysis.


SUPPORT INFORMATION AVAILABLE

Water content of the NADES studies determined through Karl Fischer.

Molar heat capacities ($C_p$) of NADES

Measured vaporization rate of hexadecane together with corresponding vapor pressures

Calibration curve using hexadecane.

Measured vaporization rate, calculated *v* and vapor pressure of different NADES

ABBREVIATIONS

| | |
|---|---|
| DES | deep eutectic solvents |
| NADES | natural deep eutectic solvents |
| La | lactic acid |
| Ma | malic acid |
| Bet | betaine |
| Pro | proline |
| Hist | histidine |
| DSC | Differential scanning calorimetry |
| TGA | Thermogravimetric analysis |
| IL | Ionic liquids |
| $\sigma$ | electrical conductivity (μS/cm) |
| $\eta$ | viscosity (Pa.s) |
| $E_\eta$ | flow activation energy (kJ/mol) |
| $E_\sigma$ | activation energy for electrical conduction (kJ/mol) |
| AAD | average absolute deviation |
| CR | crystallinity reduction (%) |
| CI | crystallinity index (%) |
| $Cp$ | molar heat capacity (J $mol^{-1}$ $K^{-1}$) |
| $C_{p,i}^{\exp}$ | experimental molar heat capacity (J $mol^{-1}$ $K^{-1}$) |
| $C_{p,i}^{\mathrm{pred}}$ | model predicted molar heat capacity (J $mol^{-1}$ $K^{-1}$) |
| R | gas constant |
| T | temperature (K) |
| $T_{av}$ | average temperature (K) |

| | |
|---|---|
| $T_0$ | arbitrarily chosen reference temperature (K) |
| $a_i$ | model parameters |
| N | number of experimental measurements |
| A’ | constant |
| P | vapor pressure (Pa) |
| M | molar mass (g $mol^{-1}$) |
| $\alpha$ | vaporization coefficient |
| *K* | constant |

REFERENCES


1. Espino, M., de los Ángeles Fernández, M., Gomez, F. J. V & Silva, M. F. Natural designer solvents for greening analytical chemistry. *Trends Anal. Chem.* **76,** 126–136 (2016).

2. Khandelwal, S., Tailor, Y. K. & Kumar, M. Deep eutectic solvents (DESs) as eco-friendly and sustainable solvent/catalyst systems in organic transformations. *J. Mol. Liq.* **215,** 345–386 (2016).

3. Dai, Y., van Spronsen, J., Witkamp, G.-J., Verpoorte, R. & Choi, Y. H. Natural deep eutectic solvents as new potential media for green technology. *Anal. Chim. Acta* **766,** 61–8 (2013).

4. Jessop, P. G., Jessop, D. A., Fu, D. & Phan, L. Solvatochromic parameters for solvents of interest in green chemistry. *Green Chem.* **14,** 1245–1259 (2012).

5. Kudłak, B., Owczarek, K. & Namieśnik, J. Selected issues related to the toxicity of ionic liquids and deep eutectic solvents—a review. *Environ. Sci. Pollut. Res.* **22,** 11975–11992 (2015).

6. Hayyan, M. *et al.* Natural deep eutectic solvents: cytotoxic profile. *Springerplus* **5,** 1–12 (2016).

7. Cvjetko Bubalo, M., Vidović, S., Radojčić Redovniković, I. & Jokić, S. Green solvents for green technologies. *J. Chem. Technol. Biotechnol.* **90,** 1631–1639 (2015).

8. Paiva, A. *et al.* Natural deep eutectic solvents–solvents for the 21st century. *ACS Sustain. Chem. Eng.* **2,** 1063–1071 (2014).

9. Duan, L., Dou, L.-L., Guo, L., Li, P. & Liu, E.-H. Comprehensive evaluation of deep

eutectic solvents in extraction of bioactive natural products. *ACS Sustain. Chem. Eng.* **4,** 2405–2411 (2016).

10. Zhang, Q. *et al.* Deep eutectic solvents: syntheses, properties and applications. *Chem. Soc. Rev.* **41,** 7108–7146 (2012).

11. Smith, E. L., Abbott, A. P. & Ryder, K. S. Deep eutectic solvents (DESs) and their applications. *Chem. Rev.* **114,** 11060–82 (2014).

12. Xin, R. *et al.* A functional natural deep eutectic solvent based on trehalose: Structural and physicochemical properties. *Food Chem.* **217,** 560–567 (2017).

13. Abbott, A. P., Capper, G. & Gray, S. Design of Improved Deep Eutectic Solvents Using Hole Theory. *ChemPhysChem* **7,** 803–806 (2006).

14. Zhang, Q., De, K., Vigier, O., Royer, S. & Jeoe, F. Deep eutectic solvents: syntheses, properties and applications. *Chem. Soc. Rev. Chem. Soc. Rev* **41,** 7108–7146 (2012).

15. Dai, Y., Van Spronsen, J., Witkamp, G. J., Verpoorte, R. & Choi, Y. H. Ionic liquids and deep eutectic solvents in natural products research: Mixtures of solids as extraction solvents. *J. Nat. Prod.* **76,** 2162–2173 (2013).

16. Tang, B. & Row, K. H. Recent developments in deep eutectic solvents in chemical sciences. *Monatshefte fur Chemie* **144,** 1427–1454 (2013).

17. Craveiro, R. *et al.* Properties and thermal behavior of natural deep eutectic solvents. *J. Mol. Liq.* **215,** 534–540 (2016).

18. Hayyan, M. *et al.* Are deep eutectic solvents benign or toxic? *Chemosphere* **90,** 2193–2195

(2013).

19. Zhang, Y., Lu, X. H., Feng, X., Shi, Y. J. & Ji, X. Y. Properties and Applications of Choline-Based Deep Eutectic Solvents. *Progress in Chemistry* (2013). doi:10.7536/PC121044

20. Radošević, K. *et al.* Natural deep eutectic solvents as beneficial extractants for enhancement of plant extracts bioactivity. *LWT - Food Sci. Technol.* **73,** 45–51 (2016).

21. Cvjetko Bubalo, M., Ćurko, N., Tomašević, M., Kovačević Ganić, K. & Radojčić Redovniković, I. Green extraction of grape skin phenolics by using deep eutectic solvents. *Food Chem.* **200,** 159–166 (2016).

22. Figueiredo, M. *et al.* Differential capacity of a deep eutectic solvent based on choline chloride and glycerol on solid electrodes. *Electrochim. Acta* **54,** 2630–2634 (2009).

23. Nkuku, C. A. & LeSuer, R. J. Electrochemistry in deep eutectic solvents. *J. Phys. Chem. B* **111,** 13271–13277 (2007).

24. Durand, E. *et al.* Evaluation of deep eutectic solvent–water binary mixtures for lipase-catalyzed lipophilization of phenolic acids. *Green Chem.* **15,** 2275–2282 (2013).

25. Zhao, H., Baker, G. A. & Holmes, S. Protease activation in glycerol-based deep eutectic solvents. *J. Mol. Catal. B Enzym.* **72,** 163–167 (2011).

26. Durand, E. *et al.* Evaluation of deep eutectic solvents as new media for Candida antarctica B lipase catalyzed reactions. *Process Biochem.* **47,** 2081–2089 (2012).

27. Stepankova, V. *et al.* Strategies for stabilization of enzymes in organic solvents. *ACS Catal.* **3,** 2823–2836 (2013).

28. Ren, H., Chen, C., Wang, Q., Zhao, D. & Guo, S. The properties of choline chloride-based deep eutectic solvents and their performance in the dissolution of cellulose. *BioResources* **11,** 5435–5451 (2016).

29. Francisco, M., van den Bruinhorst, A. & Kroon, M. C. New natural and renewable low transition temperature mixtures (LTTMs): screening as solvents for lignocellulosic biomass processing. *Green Chemistry* **14,** 2153 (2012).

30. Chiu, L.-F. F., Liu, H.-F. F. & Li, M.-H. H. Heat Capacity of Alkanolamines by Differential Scanning Calorimetry. *J. Chem. Eng. Data* **44,** 631–636 (1999).

31. Verevkin, S. P., Ralys, R. V., Zaitsau, D. H., Emel'yanenko, V. N. & Schick, C. Express thermo-gravimetric method for the vaporization enthalpies appraisal for very low volatile molecular and ionic compounds. *Thermochim. Acta* **538,** 55–62 (2012).

32. Verevkin, S. P. *et al.* Vaporization enthalpies of imidazolium based ionic liquids. A thermogravimetric study of the alkyl chain length dependence. *J. Chem. Thermodyn.* **54,** 433–437 (2012).

33. Shahbaz, K. *et al.* Thermogravimetric measurement of deep eutectic solvents vapor pressure. *J. Mol. Liq.* **222,** 61–66 (2016).

34. Park, S., Baker, J. O., Himmel, M. E., Parilla, P. A. & Johnson, D. K. Cellulose crystallinity index: measurement techniques and their impact on interpreting cellulase performance. *Biotechnol. Biofuels* **3,** 10 (2010).

35. Aissaoui, T., AlNashef, I. M. & Benguerba, Y. Dehydration of natural gas using choline chloride based deep eutectic solvents: COSMO-RS prediction. *J. Nat. Gas Sci. Eng.* **30,**

571–577 (2016).

36. Chemat, F., Anjum, H., Shariff, A. M., Kumar, P. & Murugesan, T. Thermal and physical properties of (Choline chloride+urea+l-arginine) deep eutectic solvents. *J. Mol. Liq.* **218,** 301–308 (2016).

37. Chemat, F., You, H. J., Muthukumar, K. & Murugesan, T. Effect of l-arginine on the physical properties of choline chloride and glycerol based deep eutectic solvents. *J. Mol. Liq.* **212,** 605–611 (2015).

38. Durand, E., Lecomte, J. & Villeneuve, P. Deep eutectic solvents: Synthesis, application, and focus on lipase-catalyzed reactions. *Eur. J. Lipid Sci. Technol.* **115,** 379–385 (2013).

39. Dai, Y., Witkamp, G. J., Verpoorte, R. & Choi, Y. H. Tailoring properties of natural deep eutectic solvents with water to facilitate their applications. *Food Chem.* **187,** 14–19 (2015).

40. Zubeir, L. F., Lacroix, M. H. M. & Kroon, M. C. Low transition temperature mixtures as innovative and sustainable CO2 capture solvents. *J. Phys. Chem. B* **118,** 14429–14441 (2014).

41. van Osch, D. J. G. P., Zubeir, L. F., van den Bruinhorst, A., Rocha, M. A. A. & Kroon, M. C. Hydrophobic deep eutectic solvents as water-immiscible extractants. *Green Chem.* **17,** 4518–4521 (2015).

42. Zubeir, L. F. *et al.* Thermophysical properties of imidazolium tricyanomethanide ionic liquids: experiments and molecular simulation. *Phys. Chem. Chem. Phys.* **18,** 23121–23138 (2016).

43. Abdullah, G. H. & Kadhom, M. A. Studying of two choline chloride's deep eutectic solvents

in their aqueous mixtures. *Int. J. Eng. Res. Dev.* **12,** 2278–67 (2016).

44. Zhekenov, T., Toksanbayev, N., Kazakbayeva, Z., Shah, D. & Mjalli, F. S. Formation of type III Deep Eutectic Solvents and effect of water on their intermolecular interactions. *Fluid Phase Equilib.* **441,** 43–48 (2017).

45. Siongco, K. R., Leron, R. B., Caparanga, A. R. & Li, M.-H. Molar heat capacities and electrical conductivities of two ammonium-based deep eutectic solvents and their aqueous solutions. *Thermochim. Acta* **566,** 50–56 (2013).

46. Protsenko, V. S., Kityk, A. A., Shaiderov, D. A. & Danilov, F. I. Effect of water content on physicochemical properties and electrochemical behavior of ionic liquids containing choline chloride, ethylene glycol and hydrated nickel chloride. *J. Mol. Liq. J.* **212,** 716–722 (2015).

47. Aroso, I. M. *et al.* Natural deep eutectic solvents from choline chloride and betaine – Physicochemical properties. *J. Mol. Liq.* **241,** 654–661 (2017).

48. Zhu, J. *et al.* Physicochemical properties of deep eutectic solvents formed by choline chloride and phenolic compounds at T = (293.15 to 333.15) K: The influence of electronic effect of substitution group. *J. ofMolecular Liq.* **232,** 182–187 (2017).

49. Baokou, X. & Anouti, M. Physical properties of a new deep eutectic solvent based on a sulfonium ionic liquid as a suitable electrolyte for electric double-layer capacitors. *J. Phys. Chem. C* **119,** 970–979 (2015).

50. Ma, C. *et al.* Molar Enthalpy of Mixing for Choline Chloride/Urea Deep Eutectic Solvent + Water System. *J. Chem. Eng. Data* **61,** 4172–4177 (2016).

51. Naser, J., Mjalli, F. S. & Gano, Z. S. Molar Heat Capacity of Selected Type III Deep Eutectic Solvents. *J. Chem. Eng. Data* **61,** 1608–1615 (2016).

52. Leron, R. B. & Li, M.-H. H. Molar heat capacities of choline chloride-based deep eutectic solvents and their binary mixtures with water. *Thermochim. Acta* **530,** 52–57 (2012).

53. Yu, Y.-H., Soriano, A. N. & Li, M.-H. Heat capacities and electrical conductivities of 1-ethyl-3-methylimidazolium-based ionic liquids. *J. Chem. Thermodyn.* **41,** 103–108 (2009).

54. Price, D. M. Vapor pressure determination by thermogravimetry. *Thermochim. Acta* **367–368,** 253–262 (2001).

55. Wu, S. H., Caparanga, A. R., Leron, R. B. & Li, M. H. Vapor pressure of aqueous choline chloride-based deep eutectic solvents (ethaline, glyceline, maline and reline) at 30-70 ºC. *Thermochim. Acta* **544,** 1–5 (2012).

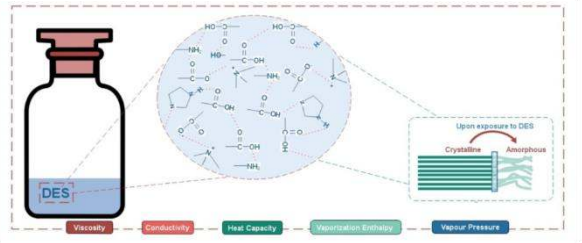


For Table of Contents Only